NRC·CNRC

NRC Publications Archive
Archives des publications du CNRC

Metallization of carbon fibre reinforced polymers by cold spray

Che, Hanqing; Vo, Phuong; Yue, Stephen

This publication could be one of several versions: author's original, accepted manuscript or the publisher's version. / La version de cette publication peut être l'une des suivantes : la version prépublication de l'auteur, la version acceptée du manuscrit ou la version de l'éditeur.
For the publisher's version, please access the DOI link below./ Pour consulter la version de l'éditeur, utilisez le lien DOI ci-dessous.

Publisher's version / Version de l'éditeur:
https://doi.org/10.1016/j.surfcoat.2017.01.083
Surface & Coatings Technology, 313, pp. 236-247, 2017-01-24

NRC Publications Archive Record / Notice des Archives des publications du CNRC :
https://nrc-publications.canada.ca/eng/view/object/?id=bc6cab07-5075-4c6e-9fee-32e32812a8cb
https://publications-cnrc.canada.ca/fra/voir/objet/?id=bc6cab07-5075-4c6e-9fee-32e32812a8cb

Access and use of this website and the material on it are subject to the Terms and Conditions set forth at
https://nrc-publications.canada.ca/eng/copyright
READ THESE TERMS AND CONDITIONS CAREFULLY BEFORE USING THIS WEBSITE.

L'accès à ce site Web et l'utilisation de son contenu sont assujettis aux conditions présentées dans le site
https://publications-cnrc.canada.ca/fra/droits
LISEZ CES CONDITIONS ATTENTIVEMENT AVANT D'UTILISER CE SITE WEB.

Questions? Contact the NRC Publications Archive team at PublicationsArchive-ArchivesPublications@nrc-cnrc.gc.ca. If you wish to email the authors directly, please see the first page of the publication for their contact information.

Vous avez des questions? Nous pouvons vous aider. Pour communiquer directement avec un auteur, consultez la première page de la revue dans laquelle son article a été publié afin de trouver ses coordonnées. Si vous n'arrivez pas à les repérer, communiquez avec nous à PublicationsArchive-ArchivesPublications@nrc-cnrc.gc.ca.

National Research Council Canada | Conseil national de recherches Canada

Canada

Surface & Coatings Technology xxx (2017) xxx-xxx

Contents lists available at ScienceDirect

Surface & Coatings Technology

journal homepage: www.elsevier.com

Metallization of carbon fibre reinforced polymers by cold spray

Hanqing Che[a,*], Phuong Vo[b], Stephen Yue[a]

[a] Department of Mining and Materials Engineering, McGill University, Montreal, H3A 0C5, Canada
[b] National Research Council Canada, Boucherville, J4B 6Y4, Canada

ARTICLE INFO

Article history:
Received 22 July 2016
Received in revised form 23 December 2016
Accepted 21 January 2017
Available online xxx

Keywords:
Metallization of polymers
Cold spray
Carbon fibre reinforced polymer

ABSTRACT

Carbon fibre reinforced polymer (CFRP) is a very competitive alternative to aluminum for aircraft structures for lightweighting purposes, but this leaves vulnerability against lightning strike. Cold spray is one coating approach to metallize the polymers, making them lightning strike proof. The aim of this work is to investigate the viability of metallizing aircraft quality CFRPs by cold spray. Copper, aluminum and tin were cold sprayed onto the CFRPs with both a high-pressure and a low-pressure cold spray system. A number of different combinations of the gas pressure and gas preheating temperature were used for the cold spray process. Erosion was found to be the key obstacle to developing continuous coatings on the CFRP substrates with the high-pressure system. On the other hand, continuous tin coatings were successfully obtained on CFRP with the low-pressure system, due to the very soft tin coating the substrate through a "crack filling" mechanism. Based on the results, it was proposed that when cold spraying metals on CFRP, it is necessary to differentiate between the development of the first layer and the build-up of subsequent layers. Last but not least, the effect of particle velocity and gas temperature was discussed and the deposition window of tin on CFRP was developed.

© 2016 Published by Elsevier Ltd.

1. Introduction

In the past a few decades, carbon fibre reinforced polymers (CFRPs) have been increasingly used in a wide range of industries due to their low density and high specific strength [1,2]. Especially in the aerospace industry, CFRPs have been extensively used for the latest generations of aircrafts and helicopters for lightweighting (e.g. Boeing 787, Airbus 350, Bombardier C-Series, etc.). However, the main drawback of replacing aluminum with CFRP is the drastic decrease in electrical conductivity (CFRPs are approximately 1000 times more resistive than aluminum to current flow [3]), which creates a serious lightning strike problem. Literature shows that an aircraft can be struck by lightning, on average, once or twice a year [4,5]. Therefore, there is an urgent need to develop lightning strike protection (LSP) solutions for the composite outer skin for the current and future generations of aircrafts, and metallization of CFRPs has attracted increasing interest during the past a few years [6–9].

To make the CFRPs electrically conductive, a conductive material must be either embedded into, or coated onto, the polymers [10]. Cold spray is one possible coating approach. Cold spray, also known as cold gas dynamic spray, is a high rate material deposition process in which powder particles are accelerated through a converging-diverging nozzle to high velocities, whereupon they impact with a substrate, deform plastically, and bond to the surface [11–13]. Because the metallic particles are deposited on a substrate as solid phase at relatively low temperature, the oxidation of sprayed materials can be minimized or prevented and the substrate heat damage is minimized; hence, cold spray is considered to be an ideal technique to fabricate electrically conductive coatings onto CFRP [9].

Up until recently, cold spray was mainly used to deposit metallic coatings onto metallic substrates. The process is well understood when spraying metallic powders onto metallic substrate surface. However, to the best knowledge of the author, only a few studies have been reported on cold spray onto polymeric substrates [9,14–19]. It has been reported that erosion of the substrates is the key problem, especially for these reinforced with carbon/glass fibres [9,14,16]. Furthermore, the thermosetting materials degrade at elevated temperature rather than softening, making it difficult to take advantage of local thermal softening of the substrates (like for thermoplastics), thus are even more difficult to obtain coatings [19]. The same should be expected for CFRPs with thermoset matrix. More investigations are needed to achieve direct cold spray onto CFRPs and to understand the deposition mechanism.

The aim of this work is to investigate the viability, and possible mechanism if viable, of metallizing CFRP by cold spray. Copper, aluminum and tin were chosen as the coating materials because of their excellent electrical and thermal conductivity, good mechanical properties, excellent cold sprayability on metal substrates and relatively low cost. Among these three materials, copper is the most conductive, and has excellent cold sprayability on metal substrates; aluminum is highly conductive and is cold sprayable on metal substrates - it is also lightweight; tin is less conductive as compared with copper and aluminum, but was reported to be most successful when cold spraying onto polymeric substrates [16,18]. Various different combinations of gas pressure and gas preheating temperature were used for the cold spray process with two commercial cold spray systems, a high-pressure system and a low-pressure system.

* Corresponding author.
Email address: hanqing.che@mail.mcgill.ca (H. Che)

http://dx.doi.org/10.1016/j.surfcoat.2017.01.083
0257-8972/© 2016 Published by Elsevier Ltd.

2. Experimental methods

The feedstock materials used in this work were commercial-purity aluminum (Valimet), spherical copper (SP, Plasma Giken), irregular copper (IR, Centerline) and tin (Centerline) powders, with average particle sizes of 25, 29, 30, and 17 μm, respectively (measured by a Horiba LA-920 laser scattering particle size distribution analyzer). The scanning electron microscope images and cross-section optical micrographs of the feedstock powders are shown in Fig. 1. The tin powder is not as spherical as the other two spherical powders; it contains the largest number of relatively small particles and has the smallest average particle size. It also shows in Fig. 1 that the IR copper has a dendritic morphology.

The carbon fibre reinforced polymer substrates used in this work are CFRP panels provided by Bombardier Aerospace (Montreal, Canada). The CFRP materials consist of a thermosetting epoxy matrix and continuous carbon fibre reinforcements. Each panel is made of four plies of Cycom 5276–1/G30–500 epoxy carbon prepreg (0/902 s). For the cold spray experiments, sheet sections of dimensions 7 × 7 cm were used as the substrates. Prior to the cold spray experiments, these sections were degreased with acetone, and no other surface preparation methods were adopted, unlike the metal substrates,

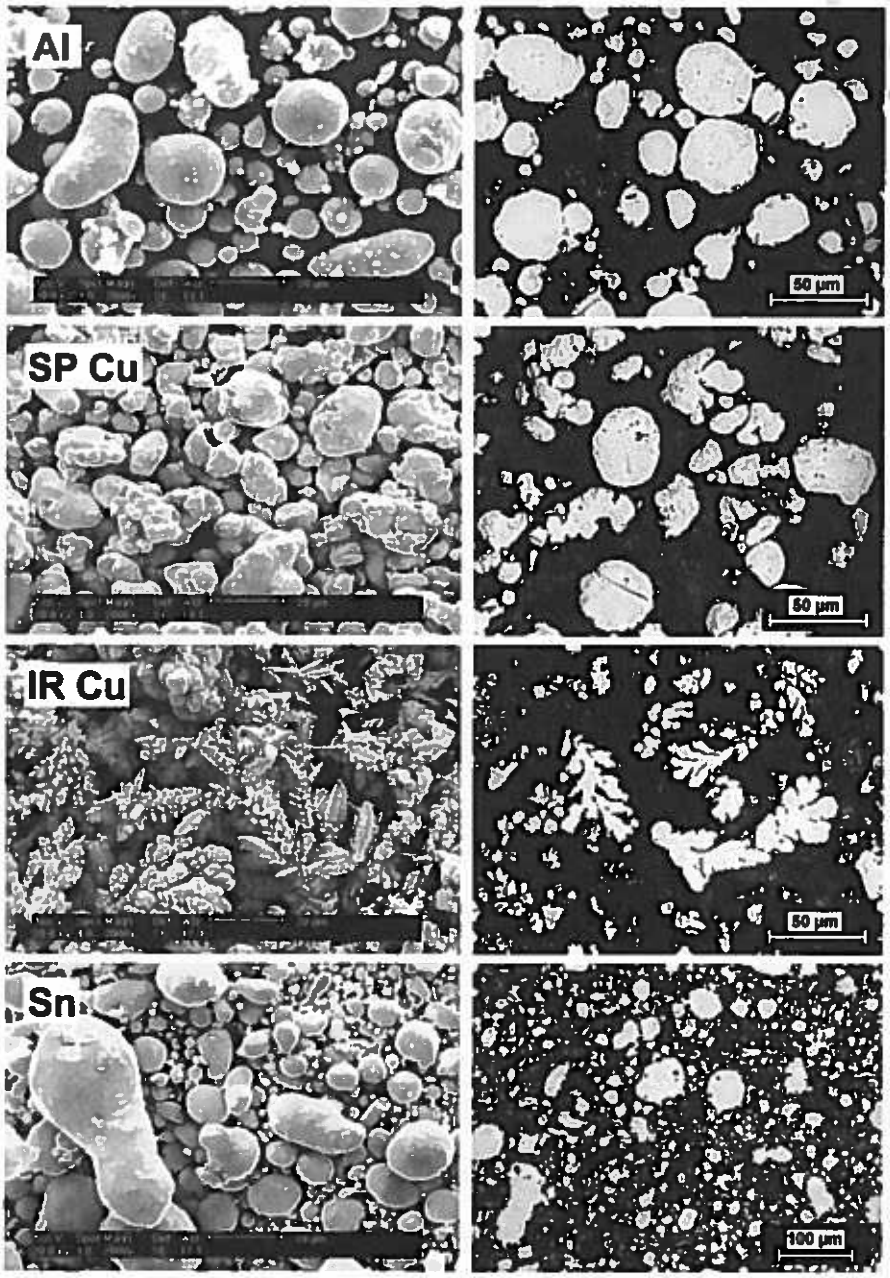

Fig. 1. SEM images (left) and cross-sectional optical micrographs (right) of the feedstock powders.

which are often grit blasted before cold spray; the CFRP substrates would be eroded during grit blasting.

Cold spray experiments were carried out at the McGill-NRC cold spray facility at National Research Council Canada, Boucherville. Both high-pressure and low-pressure cold spray experiments were performed. For high-pressure spray, a commercially available Plasma Giken PCS-800 system (Plasma Giken Co. Ltd., Japan) was used. Nitrogen was selected as the carrier gas, and four different powders were sprayed with this system at various conditions, which are shown in detail in Table 1. It should be noted that the gas temperature in Table 1 refers to the gas temperature in the converging part of the nozzle (before the throat), and is not equivalent to the particle temperature on impact. The gas temperature and gas pressure were the two primary process parameters, since they can largely influence the particle velocity, impact temperature thus the cold sprayability of one powder. The gun stand-off distance, gun travel speed and feeding rate, on the other hand, were the secondary parameters (e.g. the gun stand-off distance may affect particle velocity and temperature at impact, decreasing the gun travel speed could lead to more thermal effect, etc.). In this work, a wide range of each parameters, as listed in Table 1, were tested to achieve deposition.

A commercially available CenterLine SST system (Supersonic Spray Technologies, CenterLine Windsor Limited, Canada) was used to perform the low-pressure spray. The CenterLine system enables the so-called "downstream injection", in which the particles are introduced into the main gas stream immediately after the throat, the narrowest orifice of the nozzle, so that the risk of throat clogging in the nozzle can be alleviated. With this low-pressure system, spherical copper and tin were sprayed with nitrogen as the carrier gas, and other cold spray process parameters are listed in Table 1. Only single-layer deposition (one pass) was performed for low-pressure cold spray and the step size was set as 1 mm. Cold spray of aluminum with the low-pressure system was unsuccessful initially so it was not continued. Deposition efficiency (DE), which is the weight change of the substrate divided by the overall weight of powder sprayed out during the time that the gun is actually over the sample, was measured during the low-pressure cold spray.

The particle velocity measurements at different conditions were measured by using a ColdSprayMeter time-of-flight particle diagnostic system (Tecnar Automation, St-Bruno, QC, Canada), which uses a laser diode (7 W, $\lambda = 830$ nm) to illuminate the in-flight particles [20]. The laser was focused on the "centre" of the stream, where most particles were detected. For each measurement, a total number of 300 particles were detected.

Table 1
Process parameters for high-pressure and low-pressure cold spray.

High-pressure cold spray					
Powder	**Gas temperature °C**	**Gas pressure MPa**	**Stand-off distance mm**	**Gun travel speed mm · s^{-1}**	**Feeder setting RPM**
Al	100 to 400	2 to 5	20 to 80	300 to 500	1 to 5
SP Cu	100 to 800	2 to 5	50 to 200	50 to 500	1
IR Cu	100 to 700	2 to 5	40 to 100	300	0.5 to 5
Sn	50 to 300	1.5 to 3	40 to 200	300 to 500	1 to 8
Low-pressure cold spray					
Powder	**Gas temperature °C**	**Gas pressure MPa (psi)**	**Stand-off distance mm**	**Gun travel speed mm · s^{-1}**	**Feeding rate g/min**
SP Cu	425	0.34 to 1.38 (50 to 200)	18	25	~11
Sn	25 to 325	0.29 to 1.38 (42 to 200)	18	12.5 to 50	~13

After the cold spray experiments, the samples were characterized with a Philips XL30 FEG SEM, a Hitachi SU3500 SEM and a Nikon Epiphot 200 optical microscope equipped with a camera.

For the low-pressure cold sprayed tin coatings, the adhesion strength was assessed by performing pull-off tests, which were modified based on the ASTM C-633-01 standard. Square sections measuring approximately 1.8×1.8 cm^2 were sectioned and the coated surfaces were slightly ground in order to remove the loose particles and obtain flat surfaces. Both surfaces of the square sections were then glued to a pre-ground 6061 aluminum cylinder with a room temperature curing adhesive. The adhesion strength tests were performed using an MTS hydraulic pressure machine at a constant crosshead speed of 1.0 mm/min. For each cold spray condition, four tests were performed and the average strength was taken.

3. Results

3.1. High-pressure cold spray

For high-pressure cold spray of aluminum powder, no successful coating was obtained with all the conditions performed; erosion was found to be the key problem which prevented the development of a continuous coating. The typical microstructural images are shown in Fig. 2, in which the sample was sprayed at a gas preheating temperature of 400 °C and gas pressure of 2 MPa. The mean particle velocity (v_{50}) measured at this condition was 463 m/s, with a standard deviation of 109 m/s. This mean velocity is lower than the reported critical velocity for aluminum (520 m/s at gas temperature of 400 °C [21]), but 22% of the particles still travelled faster than the critical velocity. It can be seen clearly from Fig. 2a that there are two distinct areas in the sample, one area with the surface epoxy removed and the carbon fibres exposed as a result, and the other area with some surface epoxy left. Within the exposed carbon fibre area, fracture of the carbon fibres can be observed and no aluminum particles could be found on or among the exposed carbon fibres. A close look into the residual epoxy after erosion shows brittle fracture of the epoxy and a number of embedded particles in the eroded epoxy, as shown in Fig. 2b. Energy dispersive x-ray (EDX) mapping as shown in Fig. 2c, reveals these particles that penetrated the epoxy are aluminum. These particles remain spherical after the impact, without obvious plastic deformation. This is in contrast to the results of conventional cold spray onto metallic substrates, in which severe plastic deformation of the particles can usually be observed and adiabatic shear instability is reported to be the main mechanism of bonding [22]. It should also be noted that these embedded particles are mostly fine particles, with diameters smaller than 10 μm.

Similar to aluminum, no successful coating was achieved for cold spray of copper powders, either spherical or irregular. Once again epoxy erosion along with some embedded copper particles was found. The SEM images and cross-section micrographs of the CFRP samples after cold spray of spherical copper powder at 600 °C and 2 MPa are shown in Fig. 3. The mean particle velocity (v_{50}) measured at this condition was 548 m/s, with a standard deviation of 99 m/s. The critical velocity for copper is reported to be 460 to 500 m/s for a 20 μm particle [23], but even though more than 70% of particles at this condition travelled faster than the critical velocity, no continuous coating could not be achieved. The top surface of the sample, similar to the aluminum sample, consists of two distinct areas, the residual epoxy and the exposed carbon fibre, as shown in Fig. 3a. Although no successful coating could be achieved, embedded copper particles can be observed within the residual epoxy area from both a closer look at the top surface (Fig. 3b) as well as the cross-sectional optical

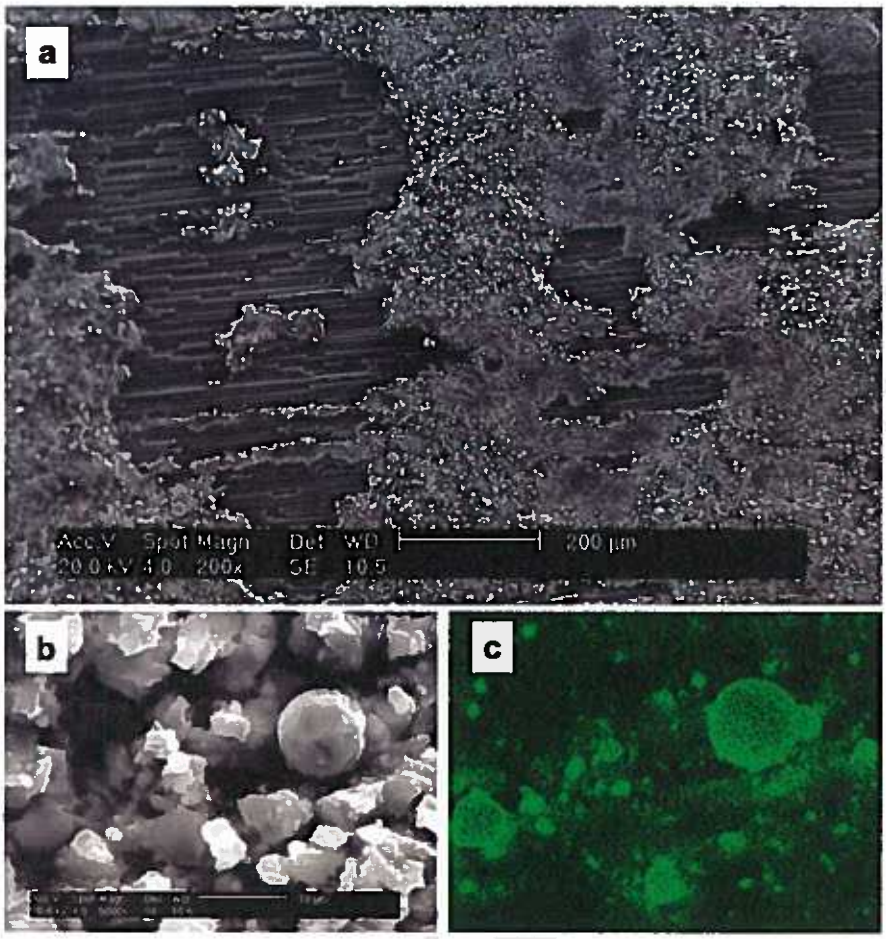

Fig. 2. SEM images (a, at low magnification and b, at high magnification) and EDX mapping (c) of the CFRP samples after cold spray of Al powder.

micrographs (Fig. 3c). These particles basically remain spherical, suggesting no obvious plastic deformation took place upon the impact on the substrates so that adiabatic shear instability was absent. More severe erosion could be found as compared to aluminum powder, since the carbon fibres were not only exposed, but also fractured after the impact of copper particles, so that a number of valleys were developed, as shown in Fig. 3d. In addition, no copper particles were deposited onto the exposed carbon fibres, which matches the results for aluminum. Cold spray of IR copper led to very similar results.

Among all four powders sprayed with the high-pressure system, cold spray of tin powder showed the most positive results, although again, no continuous coating was achieved. The microstructural images of samples sprayed at 300 °C and 1.5 MPa are shown in Fig. 4. Erosion was also the key obstacle to developing a continuous coating for spray of tin powder, despite the fact that the hardness of tin is much lower than that of aluminum or copper. Removal of the surface epoxy and exposure of the carbon fibres were also observed, but in contrast to aluminum and copper, tin could be deposited onto the exposed carbon fibres, and tin clusters can be found, as shown in Fig. 4. The cross-sectional micrograph shows clearly a thin layer of tin coating was deposited onto the carbon fibres in some local areas. No spherical particles can be observed in the cluster, indicating the particles experienced some permanent deformation during impact and building-up.

3.2. Low-pressure cold spray

For all four powders with various process conditions with high-pressure cold spray, erosion was found and is believed to be the key obstacle to developing continuous coatings. It appears that the high particle velocity in the high-pressure cold spray process leads to excessive erosion of the substrate, preventing deposition. To minimize the extent of erosion during cold spraying accordingly, a low-pressure cold spray system was used thereafter.

3.2.1. Deposition efficiency

With the low-pressure system, cold spray of spherical copper at 425 °C failed at various gas pressures assessed (50 to 200 psi or 0.34 to 1.38 MPa), with negative DE results being measured at all conditions. Erosion of the substrate occurred and dominated despite the fact that the gas pressure was relatively low.

The measured results of the deposition efficiency of tin as a function of gas preheating temperature and gas pressure are presented in Fig. 5. It can be seen that successful deposition of tin can be achieved with the low-pressure system. When the gas temperature was fixed at 300 °C, there was an abrupt increase in DE leading to a peak in DE at a gas pressure of 60 psi (0.41 MPa), as shown in Fig. 5a. The DE decreased to near zero when the gas pressure was increased to 150 psi (1.03 MPa), which is still low for conventional cold spray. On the

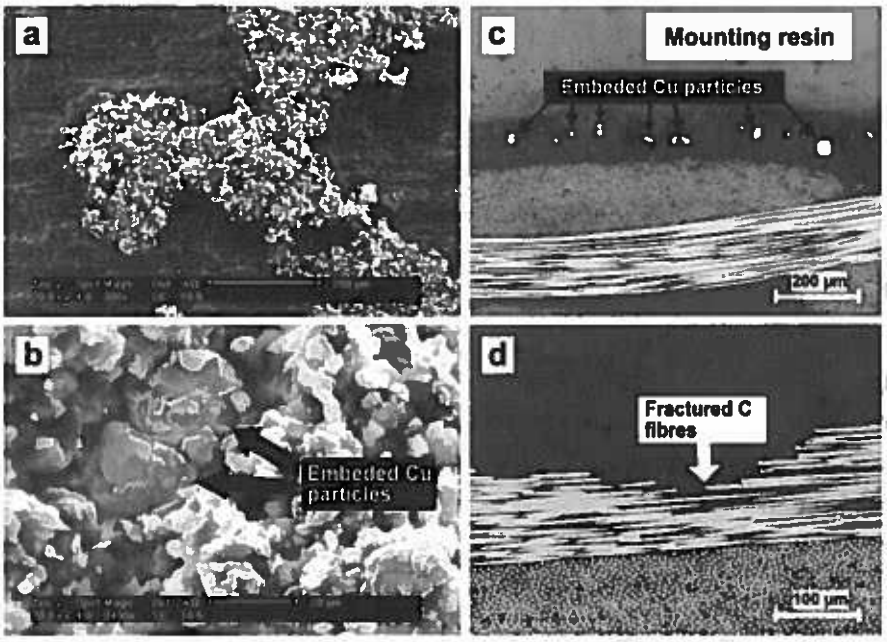

Fig. 3. SEM images (a and b) and cross-section optical micrographs (c and d) of the CFRP samples after cold spray of spherical Cu powder (the bright particles in c are copper, and the clusters of bright dots in c and d are the carbon fibres perpendicular to the observation plane).

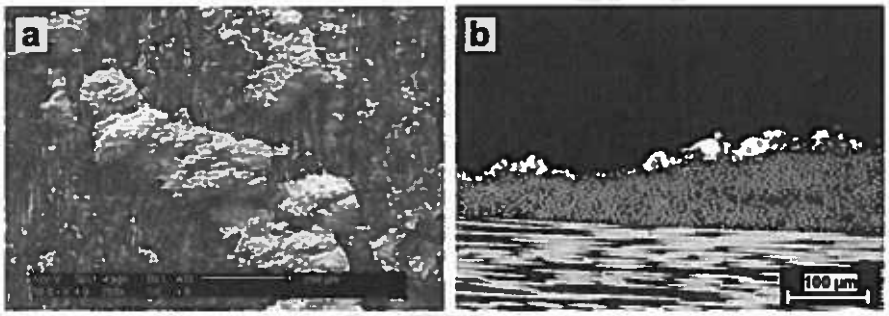

Fig. 4. SEM image (a) and cross-section optical micrograph (b) of the CFRP samples after cold spray of Sn powder (the clusters of bright dots in the cross-sectional micrograph are the carbon fibres perpendicular to the observation plane).

other hand, when the gas pressure was fixed at 60 psi, as shown in Fig. 5b, DE remained near zero at gas temperatures below 280 °C, then increased at temperatures of 280 °C and higher; there was also a dramatic increase in DE when the gas temperature was increased from 290 °C to 300 °C. The increasing trend suggests that with further increase in gas preheating temperature, DE would continue to increase, so a trial spray at 325 °C was performed, but the nozzle clogged despite the downstream injection mode was used.

The deposition efficiency results of tin at various gas pressures at 310 °C were compared with these at 300 °C, as shown in Fig. 6. It can be seen that at all four gas pressure conditions, the higher gas preheating temperature led to a higher DE. Unlike at 300 °C, there was no peak at 60 psi, but a decreasing trend through the conditions assessed as the gas pressure was increased.

3.2.2. Particle velocity

The measured mean particle velocities (v_{50}) at various conditions are shown in Fig. 7. At a gas temperature of 300 °C, as shown in Fig. 7a, v_{50} increased basically linearly with gas pressure. This agrees with the expectation that high gas pressure leads to high particle velocity. While the critical velocity for tin is reported to be 160–180 m/s assuming a 20 μm particle size [23], it can be seen that at most conditions, particles were travelling faster than this critical velocity. On the other hand, at 60 psi (0.41 MPa), the mean particle velocity did not show substantial variation from 200 °C to 310 °C, but still exhibited a slightly decreasing trend over gas temperature, as shown in Fig. 7b. This is in contrast to the expectation from the viewpoint of traditional cold spray. In general, the particle velocity increases with gas temperature in cold spray, and this has been confirmed by both experimental results and mathematical simulation [21,24,25]. Clearly, further analysis of this phenomenon is required.

3.2.3. Microstructure of the low-pressure cold sprayed tin coatings

The cross-sectional microstructures of the tin coatings deposited under different gas pressures at 300 °C are shown in Fig. 8. At 42 psi (0.29 MPa), the deposition of tin can be observed, but some uncoated area can also be found; the top surface of the CFRP remained smooth, without obvious signs of erosion. At 60 psi and 80 psi (0.41 and 0.55 MPa, respectively), the coatings were continuous, and the coating at 60 psi (Fig. 8b) is approximately twice as thick as that at

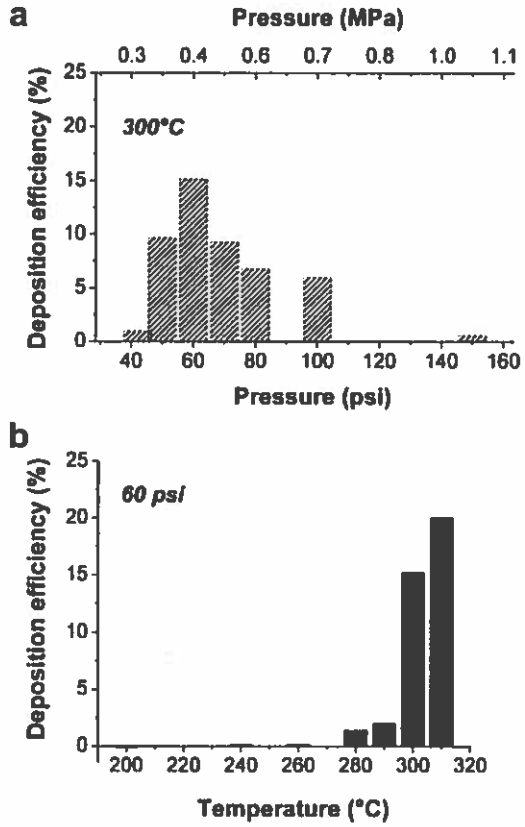

Fig. 5. Deposition efficiency of Sn as a function of gas preheating temperature when spraying at 300 °C (a) and as a function of gas pressure when spraying at 60 psi (b).

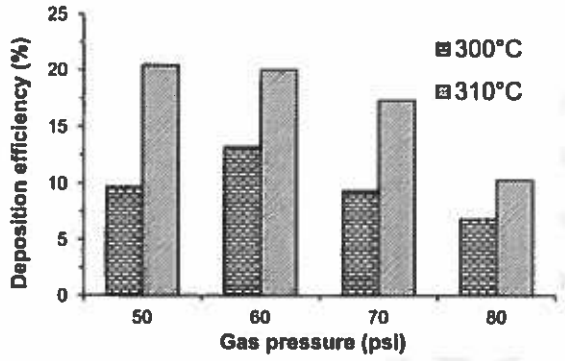

Fig. 6. Comparison of the deposition efficiency of Sn at 300 °C and at 310 °C.

80 psi (Fig. 8c), which agrees with the DE results. A close examination of the coating/substrate interfaces, as shown by the insets in Figs. 8 b and c, indicates that the particle bombardment disturbed the smoothness of the interface, leading to waviness and irregularity at the interface. In both cases, a series of tin "filaments" can be observed in the CFRP, interlocking the coatings mechanically with the substrates. However, a further increase in gas pressure led to erosion at the interface. At 150 psi (1.03 MPa), as shown in Fig. 8d, the deposition became non-continuous again, and signs of substrate erosion can be observed clearly: the surface epoxy was removed and the carbon fibres were exposed. It also shows in Fig. 8d that several tin clusters deposited directly onto the exposed carbon fibres. The substrate

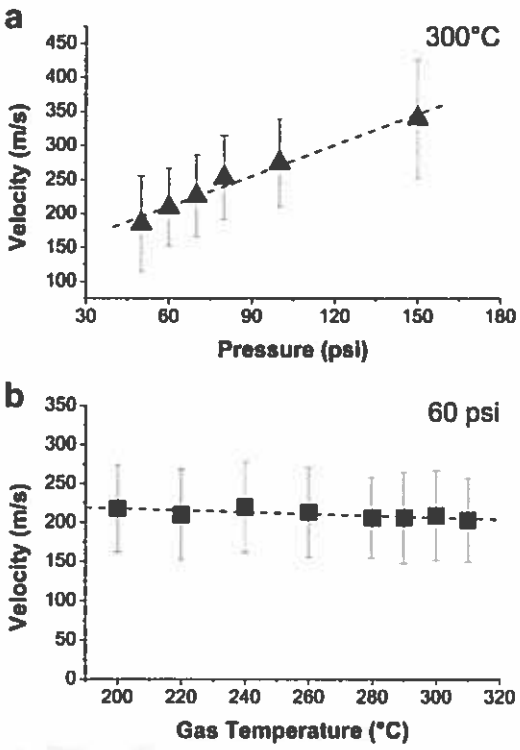

Fig. 7. The measured mean particle velocities of Sn at 300 °C (a) and 60 psi (b), the error bars represent the standard deviation.

erosion (removal) along with the cluster deposition together resulted in a near-zero DE at this condition. It can be seen that in case that deposition and erosion occur simultaneously, which cannot be differentiated from DE values, so this may lead to an underestimated DE value. However, such underestimation is usually negligible when the erosion is slight considering the relatively low density of the CFRP (~ 1.5 g/cm^3 [26])the nominal DE is underestimated.

Fig. 9 presents the top surfaces of the samples after cold spray of tin at 60 psi (0.41 MPa) at four different gas temperatures, 200 °C, 240 °C, 290 °C and 310 °C. The surface after cold spray of tin at 200 °C, at which the gas temperature was below the melting point of tin (232 °C), is shown in Fig. 9a. It can be seen that no continuous coating was deposited, although the critical velocity was reached. Fragmentation of the surface epoxy, an early sign of erosion, was also observed, but no significant removal of the epoxy occurred due to insufficient kinetic energy. A trace amount of tin can be seen within the cracks in the surface epoxy. When the gas temperature was increased to 240 °C, just above the melting point of tin, a number of small tin clusters were deposited on the CFRP, as shown in Fig. 9b. At gas temperature of 290 °C, some small areas of the CFRP were coated with a thin layer of tin, but the deposition was still non-continuous (Fig. 9c). At 310 °C, similar to 300 °C (cross section in Fig. 8b), a continuous tin coating was obtained, as shown in Fig. 9d.

To analyze the significant increase in DE at around 300 °C, a close examination of the coatings obtained at temperatures from 280 °C to 310 °C was performed. Fig. 10 shows some particles found in coatings sprayed at different temperatures. By comparing Fig. 10 a with b, it can be seen that there exists a noticeable difference between the outer surfaces of the particles found in the coatings sprayed at 280 °C and 310 °C. At 280 °C, the outer surface of the particles is relatively smooth; whereas at 310 °C, there are a large number of small "satellites" attached to the particles. These small satellites may

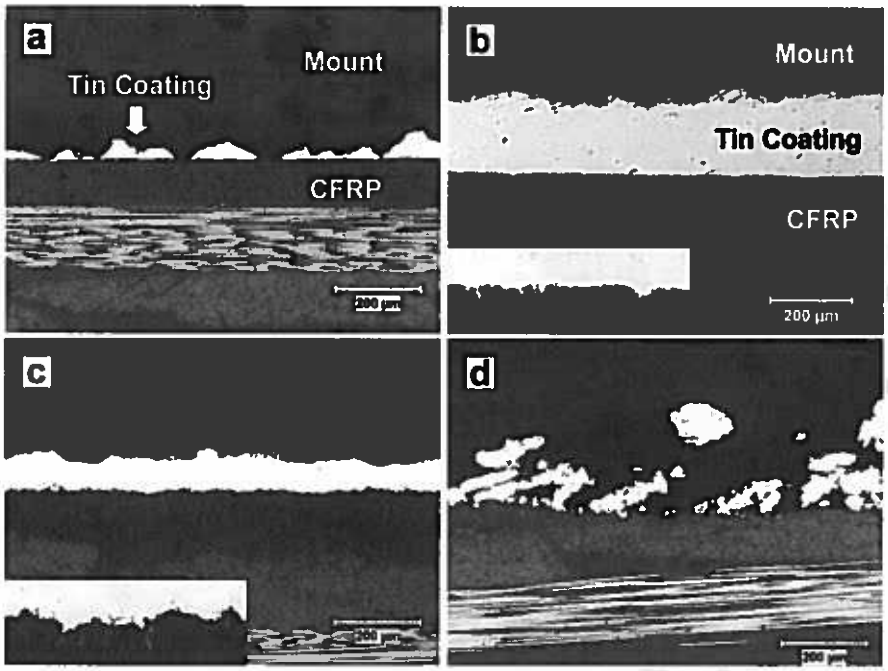

Fig. 8. Optical micrographs showing the cross-sections of cold-sprayed Sn coatings at 300 °C at 42 psi (a), 60 psi (b), 80 psi (c) and 150 psi (d), with the gun travel direction perpendicular to the observation plane; the insets in (b) and (c) show the details of the coating/CFRP interfaces.

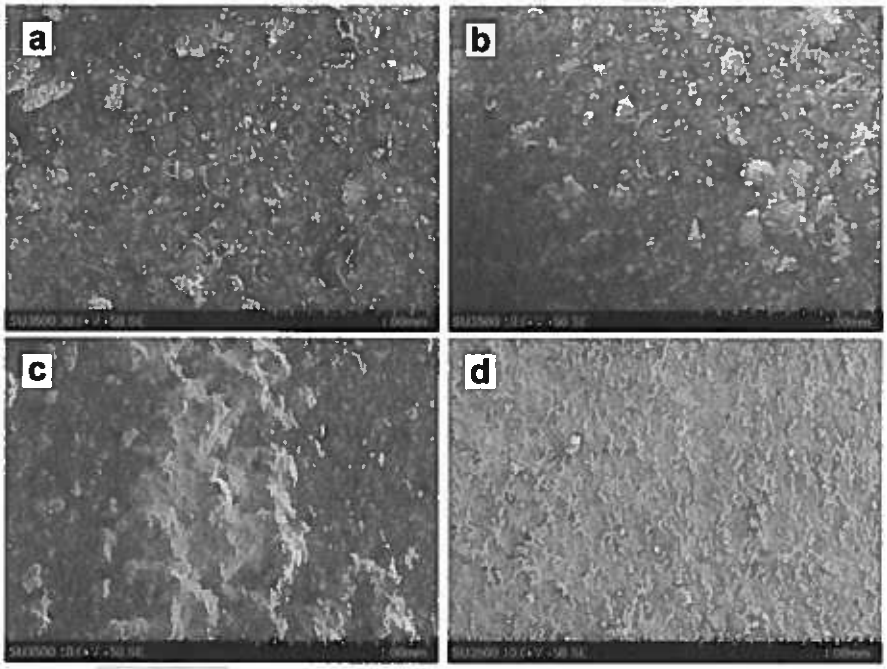

Fig. 9. SEM images showing the top surfaces of the samples after cold spray of Sn at 60 psi at 200 °C (a), 240 °C (b), 290 °C (c) and 310 °C (d), the relatively bright parts are tin and the dark parts are the CFRP.

result from splashing of the molten/partial molten tin particles during impact, considering the gas temperature is well above the melting point of tin. Fig. 10c presents a particle found in the coating sprayed at 290 °C. Similarly, the rim of this particle experienced noticeable change, as compared with the smooth surface of the starting powder. The above mentioned microstructural changes indicate that melting/partial melting of tin particle occurred. Since the change was only found in the rim/outer surface of a particle while the particle as a whole basically remained spherical, it is reasonable to believe that only the outer surface of the tin particle melted while the core remained solid. For the very fine particles, e.g. 2 to 3 µm in diameter, they could have fully melted. In general, it is not completely clear

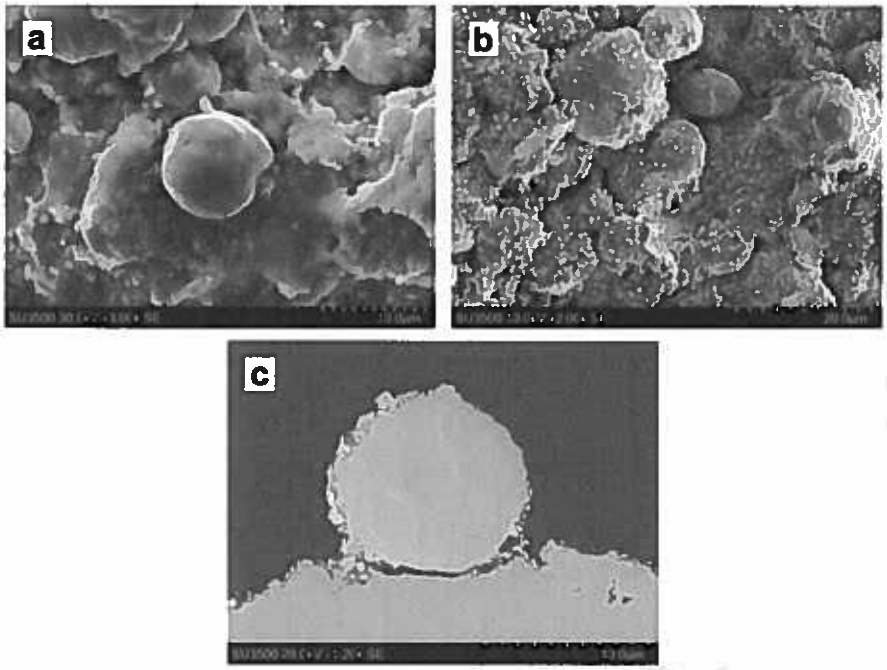

Fig. 10. SEM images showing the Sn particles at the top surfaces of coatings cold sprayed at: 280 °C (a), 310 °C (b) and 290 °C (c, cross-sectional image).

what happened, and further analysis is indeed needed to fully understand what happened during the process.

3.2.4. Adhesion tests

The adhesion test results of the tin coatings cold sprayed at various conditions are presented in Fig. 11. The tin coating cold sprayed at 300 °C and 60 psi had the strongest adhesion to the CFRP substrate, which averaged 7.6 MPa. When the gas pressure was increased to 80 psi, the adhesion strength decreased to below 3 MPa, indicating the higher kinetic energy (higher impact velocity) deteriorated the coating/substrate interlocking/interface. This is in contrast to the conventional observation that the adhesion strength basically increases with increasing particle velocity when cold spraying metals on the metal substrates [27]. This discrepancy stems from the different resistance of metals and polymeric materials to solid particle erosion. At a higher gas temperature of 310 °C, the adhesion strength of the coating cold sprayed at 60 psi was below 3 MPa, much lower than that of the coating sprayed at 300 °C. At 80 psi, the adhesion strength increased to above 4 MPa, which is also higher than that of the coating sprayed under at same pressure at 300 °C. In general, the adhesion strength of the tin coatings to the CFRP substrates was low, especially when compared with the conventional metal/metal adhesion when cold spraying onto metal substrates, and this may signify that the tin/CFRP bonding is purely mechanical.

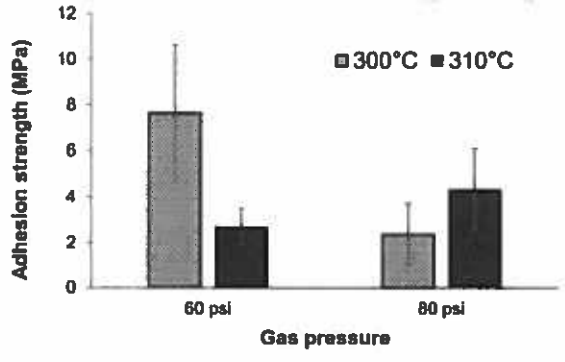

Fig. 11. Adhesion test results of the Sn coatings cold sprayed at various conditions, the error bars indicate the standard deviation.

4. Discussion

4.1. Bonding mechanism

The experimental results suggest that the conventional cold spray metrics and bonding mechanism are not directly applicable in spraying onto CFRP substrates. On the one hand, even though the particle velocity was higher than the critical velocity, deposition cannot be obtained in most cases, especially with copper and aluminum. On the other hand, except for tin clusters, the embedded metallic particles observed in this work remained spherical after impact. Without the large amount of localized plastic deformation of the particles, the conventional adiabatic shear instability mechanism for spraying metal powders onto metallic substrates is not applicable in spraying metal powders onto CFRP substrates. This discrepancy can be mainly attributed to the poor erosion resistance of the CFRP substrates, which have brittle thermosetting matrix. The critical velocities for most common metal powders are so high that the CFRP would suffer severe erosion when spraying at these velocities.

To achieve successful deposition on the CFRP, a first layer must be developed without causing unacceptable damage to the substrate surface; hereafter the conventional cold spray metrics are applicable, namely, the critical velocity must be reached and adiabatic shear instability may occur. Therefore, it is necessary to differentiate between the development of the first layer and the build-up of subsequent layers in cold spray of metals onto CFRP substrates and probably all polymeric substrates. Conversely, there is no need to consider such a differentiation when spraying onto metallic substrates, since most

metallic substrates can tolerate the high-velocity impact without significant erosion; significant erosion only occurs at excessively high velocity and it defines the upper bound of the deposition window of cold spray onto metallic substrates [23].

When developing the first metal layer onto the CFRP substrates, the most likely mechanism is mechanical interlocking, since metallurgical bonding is unlikely to form. This means the metal particles must reach a specific velocity, v_{int}, to achieve mechanical interlocking with the substrate; meanwhile, the particle velocity should not exceed an erosion limit, $v_{ero,sub}$, the velocity leading to significant substrate erosion (e.g. 50 μm removal in thickness, DE of − 2%, etc., quantification of such parameter depends largely on the substrate; noted that slight erosion of the substrate, such as micro-cracking in the substrate surface, is helpful to achieve mechanical interlocking). This brings about a relatively narrow deposition window, $v_{int} < v < v_{ero,sub}$, for developing the first metal layer on the CFRP substrates. If significant erosion of the substrate occurs before particles interlock with the substrate (i.e. $v_{ero,sub} < v_{int}$), there is no deposition, which is the case when cold spraying copper and aluminum onto CFRPs in this work. For tin, melting played an important role in achieving mechanical interlock, since continuous deposition was only achieved at high temperatures (300 °C and higher). In other words, increase in particle temperature lowers the v_{int} and thus opens the deposition window for tin.

After the first layer is developed, a critical velocity, v_{crit}, must be reached to build up subsequent layers. This is identical to the conventional cold spray of metals onto metallic substrates (only when melting occurs, v_{crit} is much smaller than in solid state). However, the possibility of coating build-up is determined/limited by the bonding strength between the first layer and the substrate. The bonding must be strong enough to withstand the bombardment of upcoming particles at velocities above v_{crit}. If the first layer is not firmly anchored, the upcoming particles can destroy the first layer, activate substrate erosion and make it impossible to build up a coating. This problem has been reported by a few researchers when trying to develop thick metallic coatings onto polymeric substrates [16,18]. Therefore, the window for coating build-up on CFRP with a previously deposited first layer is defined as $v_{crit} < v < v_{ero}$, where v_{ero} is the velocity above which the first layer can be destroyed. The magnitude of v_{ero} is dependent on the bonding strength between the first layer and the substrate as well as that between particles in the lateral direction (e.g. the continuity of the first layer, the in-plane bonding, etc.). Ideally, if a well-bonded continuous first layer is developed, v_{ero} could be the same as in conventional cold spray on metallic substrates. However, given that the mechanical interlocking between the first layer and the polymeric substrate is not expected to be very strong, v_{ero} of one powder on polymeric substrate is usually low (in most case much lower than in conventional cold spray), so only materials with relatively low v_{crit} (e.g. tin) can generate a thick coating on the CFRP substrates. In essence, these two deposition windows, $v_{int} < v < v_{ero,sub}$ and $v_{crit} < v < v_{ero}$, must be both met at the same time to make one metal powder cold sprayable onto a CFRP substrate at certain conditions. It should be noted that the deposition window varies at different gas temperatures, since the particle hardness as well as the erosion resistance of the substrate change with temperature.

In this work, the unsuccessful trials with copper and aluminum can be attributed to the failure in the development of the first layer. The copper and aluminum particles cannot achieve mechanical interlocking with the CFRP substrates, but cause brittle fragmentation and material removal in the substrate surface. Even when spraying the relatively soft tin at 200 °C, there were still difficulties in developing the first layer. When the gas temperature was increased to above 300 °C, successful coatings were finally obtained by taking advantages of partial melting of tin particles. A "crack filling" mechanism is proposed to explain the formation of the coating, as shown in Fig. 12. With this mechanism, when the tin particles enter the hot gas stream with a higher temperature than their melting point, the surface of these particles begin to melt (e.g. as shown in Fig. 10c). Due to the short residence time in the nozzle, the particles cannot wholly melt before they exit the nozzle, so the cores of particles remain solid. When these partially molten particles bombard a brittle CFRP substrate, the impact generates a number of micro-cracks in the surface epoxy. Then the molten part of the tin particles is squeezed into these cracks and solidifies, not only filling these cracks, preventing further erosion, but also achieving mechanical anchorage with the substrate and forming the first layer. Then the upcoming particles impact with this first layer and build up a coating. With this mechanism, melting is an important factor, therefore, it is inapplicable to copper and alu-

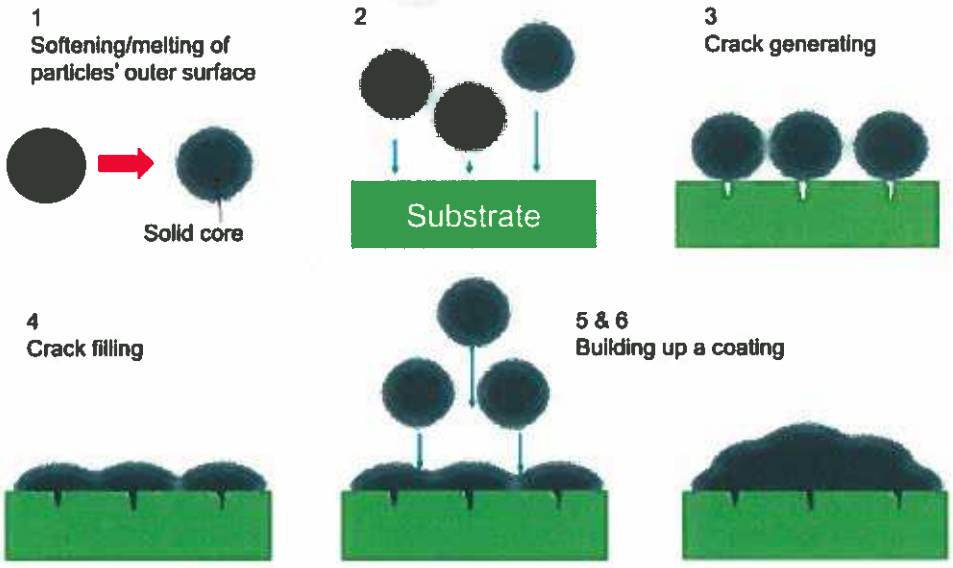

Fig. 12. Schematic of the crack filling mechanism.

minum, which have high melting points and would erode the CFRP before bonding (melting point of aluminum can be reached in some high-pressure cold spray systems, but nozzle clogging is a big problem when cold spraying aluminum near its melting point in practice).

4.2. Deposition window

4.2.1. Effect of velocity on DE

With the measured particle velocities, it is possible to plot the deposition efficiency results as a function of the mean particle velocity. Fig. 13 presents DE vs. v_{50} at three gas temperature conditions, 200 °C, 300 °C and 310 °C. The velocity measurement at 42 psi and 300 °C was unsuccessful, probably due to the low velocity being out of the range of the ColdSprayMeter, so an estimated value was used based on the linear relationship shown in Fig. 7. At gas temperature of 300 °C, deposition starts approximately at a velocity of 160 m/s and reaches a peak at around 210 m/s. With further increase in velocity, DE decreases in a gradual manner, rather than the dramatic way in which it increases, and approaches zero at 350 m/s. Similar trend can be observed at 200 °C, DE is negative at first (till at least 286 m/s), then it turns positive and reaches a maximum of 4% at 306 m/s before decreasing slightly. At 310 °C, although the ascending part of the curve wasn't experimentally determined, the descending part also shows that DE decreases with increasing velocity from a maximum.

It is understandable that DE first increases with particle velocity, since higher particle velocity would lead to more interlocking/bonding between the particles and the substrate or the previous layer. This is also true in cold spray onto metallic substrates, despite the fact that a portion of the bonding may be metallurgical bonding. However, once DE reaches a maximum, it decreases gradually and this could mainly be attributed to erosion, including both that of the substrate and that of the coating. On the one hand, increasing particle velocity can result in more erosion at the substrate surface, making deposition more retarded and more difficult. But at this stage, deposition of the particles still dominates and surpasses the erosion process, which occurs simultaneously. As a result, DE would decrease slightly and gradually with v_{50} while still remaining positive until erosion begins to dominate and DE turns negative. On the other hand, the decrease may also be caused by erosion of the tin coating by tin particles. In-process erosion of the coating rarely occurs in cold spray, but it may occur to tin due to its poor erosion resistance and low erosion limit [28,29]. Schmidt et al. [23] proposed a general schematic correlation between particle velocity and DE, and it contains a tailing decrease in DE in the high-velocity zone, which corresponds well with the gradual decrease in Fig. 13. They attributed this decrease to the erosive effects due to the "hydrodynamic penetration by the particles" known from large-scale impact dynamics [23]. The in-process erosion of the tin coating during cold spray has also been observed experimentally. Legoux et al. [30] reported that DE increased with gun travel speed when they cold sprayed tin onto steel substrate at 33 °C and 90 psi (0.6 MPa). The higher gun travel speed means less particle bombardment at the same spot, thus it indicates that more particle impact leads to a decrease in DE, and this is coincident with the effect of solid particle erosion. However, further analysis is needed to thoroughly understand the tailing in Fig. 13.

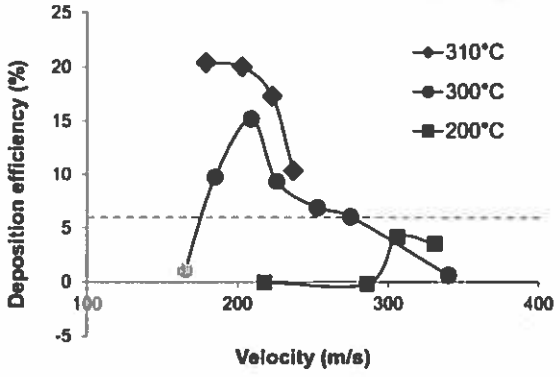

Fig. 13. Deposition efficiency of Sn at 200 °C, 300 °C and 310 °C as function of mean particle velocity (the velocity of the dotted marker is based on estimation, and the horizontal dashed line shows the onset of effective deposition).

4.2.2. Effect of temperature on DE

It can be seen from Fig. 13 that the ascending part of the DE-velocity curve shifts towards low velocities as the gas temperature increases: at 200 °C, DE remains below/near zero until 286 m/s, and reaches a maximum at a velocity of 306 m/s; at 300 °C, deposition starts approximately at 160 m/s and reaches a peak at around 210 m/s; whereas at 310 °C, deposition is projected to start at a velocity lower than 160 m/s and reach a maximum at a velocity below 180 m/s. This is because the higher gas temperature would make the metal particles more malleable (or even melt), thus easier to bond with the substrate/previous layer. This is also well known in conventional cold spray that v_{crit} decreases with higher particle temperatures [31–33]. In this work in particular, the interlocking limit, v_{int}, also decreases with temperature, since it is easier for the molten/semi-molten particles to fill the micro-cracks or interlock on the surface asperities. With decreasing v_{int} and v_{crit}, it can be understood that the ascending part of the DE-velocity curve shifts towards lower velocities at higher temperatures. As well, a higher gas temperature also results in a higher maximum DE (4%, 15% and > 20% at 200 °C, 300 °C and 310 °C, respectively). This may also be attributed to the fact that the tin particles are more malleable at higher temperatures, so that interlocking with the substrate or bonding with the previous layer is easier. Last but not least, the descending part of the DE-velocity curve has the tendency to shift to the left (low-velocity direction) as the gas temperature increases. In particular, the 300 °C curve begins to descend at a velocity well below the one at which the 200 °C curve starts to ascend. This may result from the deteriorating erosion resistance of both the tin coating and the CFRP substrate with increasing temperature [34–36].

4.2.3. Development of the deposition window as a function of particle velocity

Based on the DE-velocity relationship in Fig. 13, it is possible to determine the deposition window of tin onto CFRPs. According to Figs. 5 and 8, DE of 6% is the minimum required for a continuous coating, and can therefore be defined as the onset of effective deposition. It can be seen that the window of effective deposition when spraying tin at 300 °C onto CFRP substrates is approximately 175 to 275 m/s. At 200 °C, there is no effective deposition and thus no deposition window. At 310 °C, effective deposition of tin can be achieved, but both the lower and upper bounds of the window of effective deposition were not experimentally determined in this work. Nevertheless, it is reasonable to predict that the deposition window at 310 °C would start at a lower velocity (e.g. 150 m/s) and span a wider range of velocities assuming the DE curve follows the same trend as 300 °C (i.e. ends at approximately 290 m/s). In general, it shows clearly that higher gas temperature would lead to a higher maximum in DE, and tends to result in a wider deposition window. More data are needed to further analyze the effect of gas temperatures and particle velocity on the window of effective deposition.

For copper and aluminum, erosion of the substrate starts at low particle velocity, and begins to dominate as the particle velocity increases, leaving no possibility for depositing a coating. Thus, there is no deposition window for copper and aluminum powders when spraying onto the CFRPs.

4.2.4. Processing map

Conventionally, cold spray process deposits materials manly in solid while thermal spray usually melts the powders. In this work, some high gas temperatures (higher than the melting point of tin) were used, and it led to the melting of tin. It is, to some extent, a hybrid of thermal spray and cold spray, yet more related to cold spray. On the one hand, the particles were not fully melted and a significant portion of the particles was still solid. On the other hand, velocity is still a very important factor in this work. For conventional cold spray of metal on metal, velocity is a "method" for generating the desired thermomechanical variables (strain, strain rate and temperature) that lead to bonding. In this work, the deposition was achieved based on the combination of melting and particle velocity, which means deposition efficiency depends on both velocity and temperature.

Therefore, a semi-schematic processing map was generated for cold spray of tin on CFRP using the CenterLine system, as shown in Fig. 14. It shows the combination of variables that will lead to continuous coatings, discontinuous coatings and no coatings. In the lower left region of the map, which is the low-temperature low-pressure region, there is no deposition or erosion, due to the lack of kinetic energy and thermal softening of the particles; in the upper right area, which is the high-temperature high-pressure area, there is no coating due to significant erosion of the CFRP substrates. In the area between these two zones, being bordered by the line of deposition and the dashed line of erosion, deposition can be achieved, but continuous coatings can only be obtained inside the area marked "Continuous Coating". This continuous coating area represents the medium-pressure high-temperature area, where hot and soft particles bombard the substrates at low to medium velocities. The best conditions in terms of DE in this work (i.e. at 310 °C, 60 psi) fall into this region. This area also corresponds to the deposition windows shown in Fig. 13. Outside of the continuous coating area, the deposition is discontinuous due to either: 1) insufficient kinetic energy and thermal softening of the particles or 2) surplus kinetic energy and thermal degradation of the CFRP. At temperatures higher than 310 °C, the risk of nozzle clogging in practice is high, whereas the area below 200 °C is of little interest since the particles are not sufficiently malleable and there is no window of effective deposition.

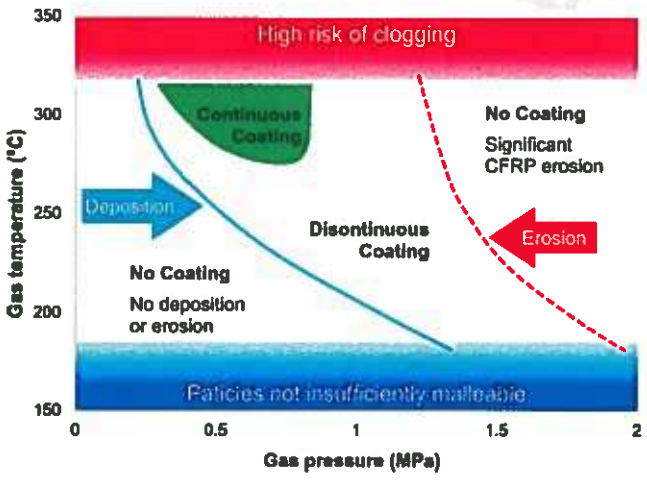

Fig. 14. Semi-schematic processing map for cold spray of Sn onto CFRP substrate.

5. Conclusions

Cold spray of aluminum, copper and tin onto CFRP were carried out. Results show that no continuous coating could be developed with various process conditions when using the high-pressure cold spray system. Erosion of the substrate was found for most conditions tested and is believed to be the key obstacle to developing continuous coatings

Continuous tin coatings were successfully obtained with the low-pressure cold spray system, whereas low-pressure cold spray of copper at various conditions still resulted in the erosion problem. Analysis of deposition efficiency indicates that medium gas pressure (around 60 psi) and high gas temperature (300 °C and higher) are required for continuous deposition of tin onto the CFRP substrates. Examination of the coating morphology and microstructure reveals that tin particles partially melted when cold sprayed at gas temperature of 300 °C and higher, and successful coatings were achieved by taking advantage of this partial melting. Accordingly, a "crack filling" mechanism was proposed to explain the deposition.

Based on the high-pressure and low-pressure cold spray results, it is necessary to differentiate the development of the first layer from the building-up of subsequent layers in cold spray of metals onto CFRP substrates. Mechanical interlocking is the most likely deposition mechanism when depositing the first metal layer on CFRP, and the conventional cold spray metrics may become applicable during the building-up of subsequent layers. Two deposition criteria were proposed, $v_{int} < v < v_{ero,sub}$ for developing the first layer and $v_{crit} < v < v_{ero}$ for the building-up. The two windows must be both met at the same time to make one metal powder cold sprayable onto a CFRP substrate at certain conditions. The deposition windows for tin were experimentally determined based on the DE-velocity relationship. It was found that cold spray of tin onto CFRP has a narrow deposition window, but higher gas temperature can result in a higher maximum DE and probably a wider deposition window.

Acknowledgement

The authors wish to acknowledge the financial support of the Consortium for Research and Innovation in Aerospace in Quebec (CRIAQ) and the Natural Sciences and Engineering Research Council of Canada (NSERC). The industrial partners, Bombardier Aerospace, and the collaborating university, École Polytechnique de Montréal, are gratefully acknowledged. Mr. Frédéric Belval and Mr. Jean-François Alarie from National Research Council Canada, Boucherville, and Dr. Huseyin Aydin from McGill University are acknowledged for their contribution to the cold spray experiments.

References

[1] M. Menningen, H. Weiss, Application of fracture mechanics to the adhesion of metal coatings on CFRP, Surf. Coat. Technol. 76 (1995) 835–840.
[2] A.B. Strong, Fundamentals of Composites Manufacturing : Materials, Methods, and Applications, second ed., Society of Manufacturing Engineers, Dearborn, 2008.
[3] U.S. Department of Transportation, Federal Aviation Administration, Aviation Maintenance Technician Handbook - Airframe Volume 1, FAA Airman Testing Standards Branch, Oklahoma City, 2012.
[4] S. Black, Lightning strike protection strategies for composite aircraft, High Perform. Compos. 21 (2013) 52–61.
[5] A. Larsson, A. Delannoy, P. Lalande, Voltage drop along a lightning channel during strikes to aircraft, Atmos. Res. 76 (2005) 377–385.

[6] G. Archambault, B. Jodoin, S. Gaydos, M. Yandouzi, Metallization of carbon fiber reinforced polymer composite by cold spray and lay-up molding processes, Surf. Coat. Technol. 300 (2016) 78–86.
[7] Z. Guo, L. Sang, Z. Wang, Q. Chen, L. Yang, Z. Liu, Deposition of copper thin films by plasma enhanced pulsed chemical vapor deposition for metallization of carbon fiber reinforced plastics, Surf. Coat. Technol. 307 (2016) 1059–1064.
[8] E. Njuhovic, A. Witt, M. Kempf, F. Wolff-Fabris, S. Glöde, V. Altstädt, Influence of the composite surface structure on the peel strength of metallized carbon fibre-reinforced epoxy, Surf. Coat. Technol. 232 (2013) 319–325.
[9] J. Affi, H. Okazaki, M. Yamada, M. Fukumoto, Fabrication of aluminum coating onto CFRP substrate by cold spray, Mater. Trans. 52 (2011) 1759–1763.
[10] G. Gardiner, Lightning Strike Protection for Composite Structures, High Perform, Compos, July, 2006.
[11] T. Hussain, D.G. McCartney, P.H. Shipway, D. Zhang, Bonding mechanisms in cold spraying: the contributions of metallurgical and mechanical components, J. Therm. Spray Technol. 18 (2009) 364–379.
[12] A.P. Alkhimov, V.F. Kosarev, A.N. Papyrin, A method of cold gas-dynamic deposition, Soviet Physics Doklady 35 (1990) 1047–1049.
[13] A. Papyrin, V. Kosarev, S. Klinkov, A. Alkhimov, V.M. Fomin, Cold Spray Technology, Elsevier, Oxford, 2007.
[14] D. Zhang, P.H. Shipway, D.G. McCartney, Cold gas dynamic spraying of aluminum: the role of substrate characteristics in deposit formation, J. Therm. Spray Technol. 14 (2005) 109–116.
[15] A. Sturgeon, B. Dunn, S. Celotto, W. O'Neill, Cold Sprayed Coatings for Polymer Composite Substrate, in: B. Battrick (Ed.), Proceedings of the 10th ISMSE, 8th ICPMSE, Collioure, France, 2006.
[16] R. Lupoi, W. O'Neill, Deposition of metallic coatings on polymer surfaces using cold spray, Surf. Coat. Technol. 205 (2010) 2167–2173.
[17] X.L. Zhou, A.F. Chen, J.C. Liu, X.K. Wu, J.S. Zhang, Preparation of metallic coatings on polymer matrix composites by cold spray, Surf. Coat. Technol. 206 (2011) 132–136.
[18] A. Ganesan, J. Affi, M. Yamada, M. Fukumoto, Bonding behavior studies of cold sprayed copper coating on the PVC polymer substrate, Surf. Coat. Technol. 207 (2012) 262–269.
[19] A. Ganesan, M. Yamada, M. Fukumoto, Cold spray coating deposition mechanism on the thermoplastic and thermosetting polymer substrates, J. Therm. Spray Technol. 22 (2013) 1275–1282.
[20] E. Irissou, J.-G. Legoux, B. Arsenault, C. Moreau, Investigation of Al-Al2O3 cold spray coating formation and properties, J. Therm. Spray Technol. 16 (2007) 661–668.
[21] R. Huang, H. Fukanuma, The influence of Spray Conditions on Deposition Characteristics of Aluminum Coatings in Cold Spraying, in: B.R. Marple, M.M. Hyland, Y.-C. Lau, C.-J. Li, R.S. *lima*, G. Montavon (Eds.) International Thermal Spray Conference, Las Vegas 2009.
[22] H. Assadi, F. Gartner, T. Stoltenhoff, H. Kreye, Bonding mechanism in cold gas spraying, Acta Mater. 51 (2003) 4379–4394.
[23] T. Schmidt, H. Assadi, F. Gärtner, H. Richter, T. Stoltenhoff, H. Kreye, T. Klassen, From particle acceleration to impact and bonding in cold spraying, J. Therm. Spray Technol. 18 (2009) 794–808.
[24] V.K. Champagne, D.J. Helfritch, S.P.G. Dinavahi, P.F. Leyman, Theoretical and experimental particle velocity in cold spray, J. Therm. Spray Technol. 20 (2011) 425–431.
[25] P.L. Fauchais, J.V.R. Heberlein, M.I. Boulos, Thermal Spray Fundamentals : From Powder to Part, Springer US, Boston, 2014.
[26] L. Cheng, G.Y. Tian, Surface crack detection for carbon fiber reinforced plastic (CFRP) materials using pulsed eddy current thermography, IEEE Sensors J. 11 (2011) 3261–3268.
[27] R. Huang, H. Fukanuma, Study of the influence of particle velocity on adhesive strength of cold spray deposits, J. Therm. Spray Technol. 21 (2012) 541–549.
[28] D. Rickerby, Correlation of erosion with mechanical properties in metals, Wear 84 (1983) 393–395.
[29] T. Schmidt, F. Gärtner, H. Assadi, H. Kreye, Development of a generalized parameter window for cold spray deposition, Acta Mater. 54 (2006) 729–742.
[30] J.-G. Legoux, E. Irissou, C. Moreau, Effect of substrate temperature on the formation mechanism of cold-sprayed aluminum, zinc and tin coatings, J. Therm. Spray Technol. 16 (2007) 619–626.
[31] C.-J. Li, W.-Y. Li, H. Liao, Examination of the critical velocity for deposition of particles in cold spraying, J. Therm. Spray Technol. 15 (2006) 212–222.
[32] T. Schmidt, F. Gaertner, H. Kreye, New developments in cold spray based on higher gas and particle temperatures, J. Therm. Spray Technol. 15 (2006) 488–494.
[33] K. Yokoyama, M. Watanabe, S. Kuroda, Y. Gotoh, T. Schmidt, F. Gärtner, Simulation of solid particle impact behavior for spray processes, Mater. Trans. 47 (2006) 1697–1702.
[34] M. Ivosevic, R. Knight, S.R. Kalidindi, G.R. Palmese, J.K. Sutter, Solid particle erosion resistance of thermally sprayed functionally graded coatings for polymer matrix composites, Surf. Coat. Technol. 200 (2006) 5145–5151.
[35] A. Patnaik, A. Satapathy, N. Chand, N. Barkoula, S. Biswas, Solid particle erosion wear characteristics of fiber and particulate filled polymer composites: a review, Wear 268 (2010) 249–263.
[36] G. Sundararajan, M. Roy, Solid particle erosion behaviour of metallic materials at room and elevated temperatures, Tribol. Int. 30 (1997) 339–359.

UNCORRECTED